

spectroscopy turns out to be an extremely structurally sensitive method.

In conclusion, we can state that electron energy-loss spectroscopy has proved to be an excellent experimental device for determining and picturing the structural and electronic details of a compound. Here, in combination with theoretical calculations at the "full potential" level, it is more convincing than any other method, such as X-ray or neutron diffraction. In the case of two metal diboride–dicarbides, contradictory notions about the arrangement of boron and carbon atoms could thus be arbitrated by combining the methods of diffraction, DFT calculations, and EELS. Contrary to what was once assumed, CaB_2C_2 and LaB_2C_2 are not isotypic.

We are indebted to Prof. Dr. Reginald Gruehn, the Deutsche Forschungsgemeinschaft, and the Fonds der Chemischen Industrie for supporting this research.

- [1] T. Bréant, D. Pensec, J. Bauer, J. C. Debuigne, *C. R. Seances Acad. Sci.* **1978**, 287, 261–264.
 [2] J. Bauer, O. Bars, *Acta Crystallogr.* **1980**, B36, 1540–1544.
 [3] J. K. Burdett, E. Canadell, T. Hughbanks, *J. Am. Chem. Soc.* **1986**, 108, 3971–3976.
 [4] B. Albert, K. Schmitt, *Inorg. Chem.* **1999**, 38, 6159–6163.
 [5] T. Onimaru, H. Onodera, K. Ohoyama, M. Ohashi, Y. Yamaguchi, *J. Phys. Chem. Solids* **1999**, 60, 1435–1438.
 [6] J. van Duijn, K. Suzuki, J. P. Attfield, *Angew. Chem.* **2000**, 112, 373–374; *Angew. Chem. Int. Ed.* **2000**, 39, 365–366.
 [7] J. Akimitsu, K. Takenawa, K. Suzuki, H. Harima, Y. Kuramoto, *Science* **2001**, 293, 1125–1126.
 [8] R. F. Egerton, *Electron Energy Loss Spectroscopy in the Electron Microscope*, 2nd. ed., Plenum Press, New York, NY, **1996**.
 [9] H. Sauer, R. Brydson, P. N. Rowley, W. Engel, J. M. Thomas, *Ultramicroscopy* **1993**, 49, 198–209.
 [10] K. Hofmann, R. Gruehn, B. Albert, *Z. Anorg. Allg. Chem.* **2002**, 2691–2696.
 [11] M. Nelhiebel, P.-H. Louf, P. Schattschneider, P. Blaha, K. Schwarz, B. Jouffrey, *Phys. Rev. B* **1999**, 59, 12807–12814.
 [12] P. Blaha, K. Schwarz, J. Luitz, *WIEN97, A Full Potential Linearized Augmented Plane Wave Package for Calculating Crystal Properties*, K. Schwarz, Technische Universität Wien, Austria, **1999**.

Received: July 4, 2002 [Z 450]

Chemically Assembled Single-Wall Carbon Nanotubes and their Electrochemistry

Peng Diao, Zhongfan Liu,* Bin Wu, Xiaolin Nan, Jin Zhang, and Zhong Wei^[a]

KEYWORDS:

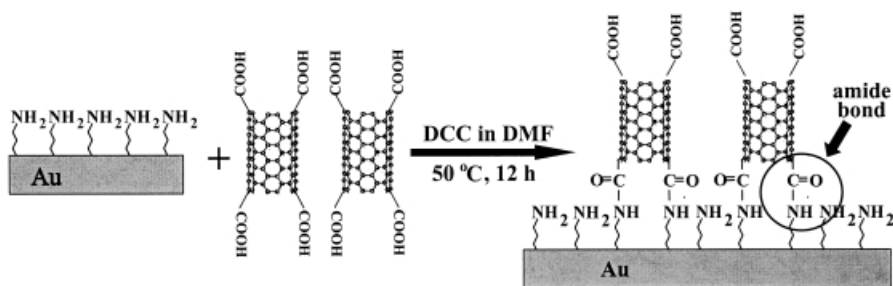
condensation · cyclic voltammetry · electrochemistry · nanotubes · self-assembly

Single-wall carbon nanotubes (SWNTs) have attracted great interest because of their unique structural, mechanical, and electronic properties. Recent studies have shown that SWNTs may have potential applications in diverse fields, for example in nanodevices,^[1] sensors,^[2] and scanning probes.^[3] The ability to prepare highly oriented SWNT arrays is crucial for improving the performance of these devices. Recently, Papadimitrakopoulos et al. and our group reported the formation of short SWNT assemblies oriented normal to the substrate through surface reactions.^[4] This finding makes the study on the properties of the aligned SWNTs possible. Knowledge of the electrochemical properties of the aligned SWNT assemblies is essential with respect to their potential applications in developing scanning electrochemical microscopy,^[5] designing electrochemical and bioelectrochemical sensors,^[6] and fabricating ultramicroelectrodes arrays. However, no such studies have been reported up to now.

Herein, we report the fabrication and characterization of chemically assembled SWNTs (ca-SWNTs), which are constructed by the combination of a self-assembling procedure and a surface condensation reaction. We demonstrate that ca-SWNTs, though immobilized on insulating monolayer-coated gold substrates, are electrochemically addressable and behave like a collection of closely spaced microelectrodes. Furthermore, metals such as copper can be electrodeposited onto ca-SWNTs.

The ca-SWNT preparation strategy, which is different from our previous procedures,^[4b,c] is shown in Scheme 1. SWNTs were cut by oxidation in mixed acid under sonication. During the cutting process, the open ends of the SWNTs were modified with COOH groups.^[7] The SWNT assemblies were then prepared through a surface condensation reaction between COOH groups at the ends of shortened SWNTs and NH_2 groups at preformed 11-amino-*n*-undecylmercaptan (AUM) monolayers on Au substrates with dicyclohexylcarbodiimide (DCC) as condensing agent^[8] (DCC-assisted condensation method; Scheme 1).

[a] Prof. Dr. Z. Liu, Dr. P. Diao, Dr. B. Wu, Dr. X. Nan, Dr. J. Zhang, Dr. Z. Wei
 Center for Nanoscale Science and Technology (CNST)
 College of Chemistry and Molecular Engineering
 Peking University
 Beijing 100871 (P.R. China)
 Fax: (+86) 10-6275-7157
 E-mail: lzf@chem.pku.edu.cn



Scheme 1. Schematic representation of the formation of SWNT assemblies.

From a typical tapping mode atomic force microscopic (AFM) image of ca-SWNTs (Figure 1 a), needlelike protrusions can be seen clearly. The apparent widths of these protrusions are about tens of nanometers, which are significantly larger than the

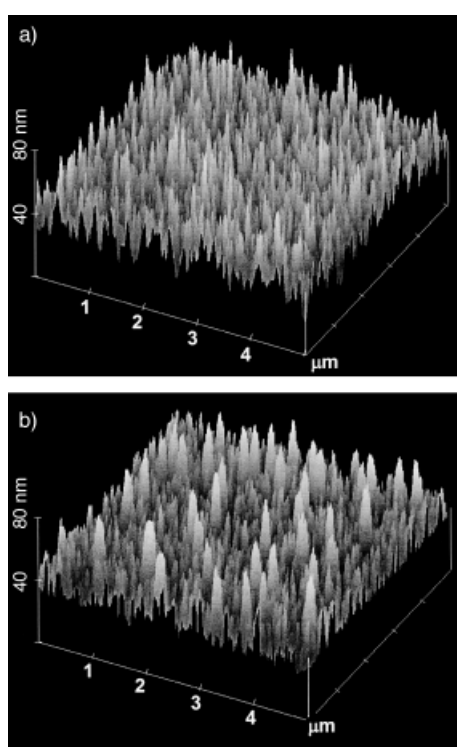


Figure 1. Tapping mode AFM images of ca-SWNTs a) before and b) after Cu deposition at -0.3 V (versus SCE) for 120 s in 0.5 M H_2SO_4 containing 1 mM $CuSO_4$.

diameter of SWNTs. We believe this is due to the tip-induced broadening artifact^[9] and SWNTs aggregating in the assembly process. The apparent protrusion height is about 10–40 nm, which is in agreement with the values obtained previously.^[4] The real height of ca-SWNTs is believed to be greater, because the curvature of the pyramidal AFM tip significantly restricts its ability to image narrow and deep features. From Figure 1 a we also notice that the density of ca-SWNTs prepared by the DCC-assisted condensation method is much higher than the density of those prepared previously on metal surfaces.^[4b,c]

Polarized Raman spectra of ca-SWNTs indicate that the Raman intensity is highest when the polarization of the incident light is parallel to the SWNT axis and greatly reduced when it is perpendicular (Figure 2). This implies that ca-SWNTs are oriented normal to the Au substrate.^[4a, 10] Because of the extremely low contrast between SWNTs and the Au substrate in SEM images, high resolution TEM was employed to investigate the orientation of ca-SWNTs prepared on

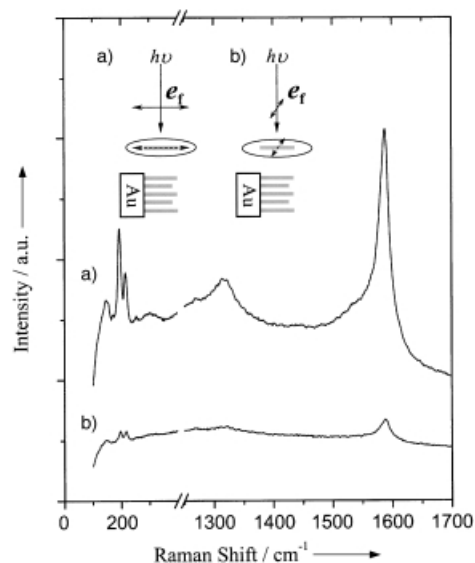


Figure 2. Polarized Raman spectra at the cross section of Au substrate coated with ca-SWNTs. The polarization of the incident light is a) parallel or b) perpendicular to the nanotube axis.

ultrathin Au wires. Results are shown in Figure 3, from which we can see that SWNTs are tethered with only one of their ends to the Au substrate. The characteristic stretching bands at 1659 and 1634 cm^{-1} ($\nu_{C=O}$) in the reflection absorption Fourier transform infrared (FTIR) spectrum (Figure 4) indicate the formation of

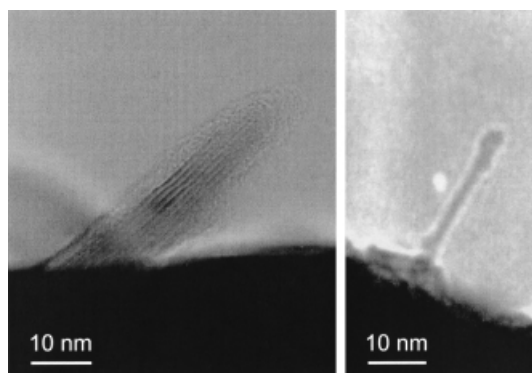


Figure 3. TEM images of SWNTs chemically assembled on an ultrathin Au wire.

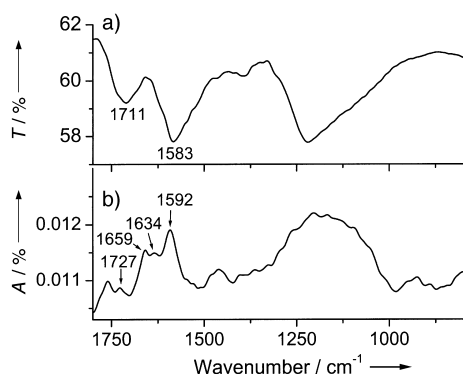


Figure 4. a) FTIR spectrum of shortened SWNTs and b) reflection absorption FTIR spectrum of ca-SWNTs.

amide bonds,^[7] which link SWNTs and the Au substrate together (see also Scheme 1).

Figure 5 shows the cyclic voltammograms (CVs) of ca-SWNT electrodes in a $[\text{Ru}(\text{NH}_3)_6]\text{Cl}_3$ solution. The redox waves observed at a bare Au electrode (curve a) are not present for an AUM coated Au electrode (Au/AUM; curve b) but return upon

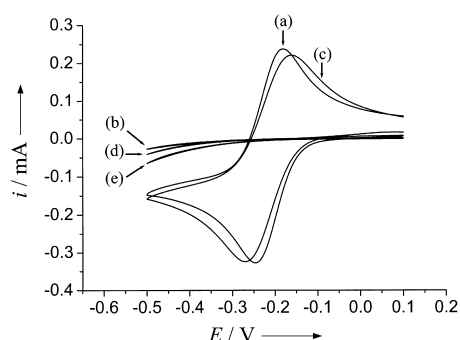


Figure 5. Cyclic voltammograms of electrodes of a) bare Au, b) Au/AUM, c) Au/AUM-SWNTs, d) Au/AUM immersed in DMF at 50 °C for 34 h, and e) Au/AUM-COOH in 1 M KCl containing 5 mM $[\text{Ru}(\text{NH}_3)_6]\text{Cl}_3$.

chemical assembly of SWNTs (Au/AUM-SWNTs; curve c). Although the size of the SWNTs is on the scale of nanometers and SWNTs are linked directly to an insulating AUM monolayer,^[11] the voltammetric behavior of Au/AUM-SWNTs resembles that of macroscopic bare Au electrode. The peak-to-peak separation of Au/AUM-SWNTs is about 100 mV at a scan rate of 100 mV s^{-1} , indicating an array of closely spaced microelectrodes.^[12] To rule out the possibility that the current waves of Au/AUM-SWNTs stem from the desorption of AUM in the surface condensation reaction, we performed electrochemical experiments using Au/AUM electrodes immersed in dimethylformamide (DMF) for 34 h at 50 °C, to see if AUM molecules desorb. The absence of redox peaks (curve d) suggests that the AUM monolayers are stable in the surface condensation reaction. Since the AUM monolayers are positively charged and hinder the redox reaction of positively charged ions, such as $[\text{Ru}(\text{NH}_3)_6]^{3+}$,^[11] the surface charge state of the AUM monolayer may influence its blocking property. Due to steric hindrance, not all COOH groups at the tethered ends of

SWNTs condense with NH_2 groups. The residue COOH groups will be ionized at neutral pH and give COO^- ions, which may change the charge state of AUM monolayers and then may result in the reappearance of current waves. To study this issue, we linked oxalic acid to the AUM monolayers by a similar condensation procedure to ca-SWNTs. Reflection absorption FTIR spectroscopy confirmed both the formation of amide bond and the presence of COOH groups (data not shown). The fact that no redox waves appear for the Au/AUM-CO-COOH electrode (curve e) indicates that the redox peaks at Au/AUM-SWNTs did not arise from the change of surface charge state of AUM monolayers. According to the above discussion, we believe that ca-SWNTs are responsible for the reappearance of current waves and that the electron transfer between Au substrate and ca-SWNTs occurs via through-bond tunneling.^[13]

The Au/AUM-SWNT electrodes can be employed for deposition of metals onto their surface. As illustrated in Figure 6, Cu^{2+} can be electrochemically reduced at bare Au electrodes (curve a)

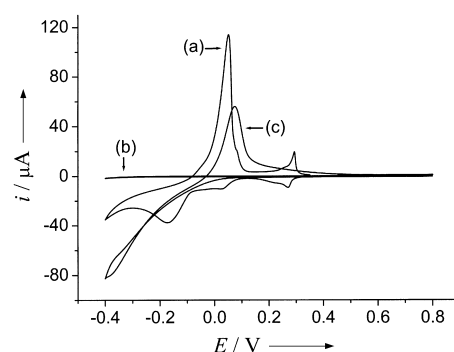


Figure 6. Cyclic voltammograms of electrodes of a) bare Au, b) Au/AUM, and c) Au/AUM-SWNTs in 0.5 M H_2SO_4 containing 1 mM CuSO_4 .

but not at Au/AUM electrodes (curve b). However, after SWNTs are chemically assembled on Au substrates, the depositing and stripping currents of Cu can be clearly observed in the negative and positive scans, respectively (curve c). The presence of Cu on SWNTs was also confirmed by XPS measurements (Figure 7). Further evidence of Cu deposition is obtained from a typical AFM

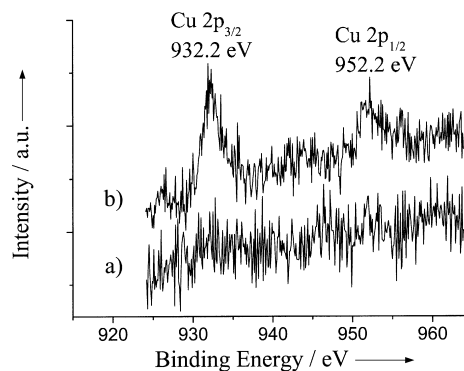


Figure 7. XPS spectra of a) Au/AUM and b) Au/AUM-SWNTs after Cu deposition at -0.3 V (versus SCE) for 120 s in 0.5 M H_2SO_4 containing 1 mM CuSO_4 .

image (Figure 1b) in which the values of the width and the height (about 20–60 nm high) of protrusions become greater compared to those before the deposition, suggesting that Cu can be deposited onto the sidewalls and ends of SWNTs. The deposition of metals on SWNTs provides a new approach to fabricating metal nanowire arrays using SWNTs as templates.

In summary, we have developed a new procedure for preparing ca-SWNTs and have demonstrated that these aligned SWNTs can be used as microelectrode arrays. The microelectrode capabilities of ca-SWNTs expand the potential applications of SWNTs in many fields, such as fabricating aligned metal nanowire arrays, preparing bioelectrochemical sensors,^[6] designing ionic or molecular recognition electrodes by functionalizing the protruding ends of ca-SWNTs, and developing multi-tip scanning electrochemical microscopes.^[5]

Experimental Section

The SWNTs used in this work were synthesized by CVD using a Fe-Mo catalyst.^[14] The purification and chemical shortening of long SWNTs followed the procedure described by Liu et al.^[15] The self-assembled monolayers of AUM on Au were prepared by immersing Au substrates in absolute ethanol containing 1 mM AUM for 24 h. The resulting film coated Au substrates were rinsed with absolute EtOH and dried in a stream of highly pure N₂. The surface condensation reaction was performed in DMF (10 mL) containing shortened SWNTs (2 mg) and DCC (5 mg). The reaction was carried out at 50 °C for 12 h.

AFM characterization was performed on a Nanoscope IIIa microscope in tapping mode. Polarized Raman spectra were recorded on a Renishaw Raman spectrometer using an excitation wavelength of 632.8 nm. To rotate the polarization of the incident laser beam, a half-wave plate was inserted before the objective of the microscope.^[10] TEM images were obtained using a Hitachi H-9000NAR TEM unit at 300 kV. FTIR spectra were measured on a Perkin–Elmer 2000 spectrometer. CV measurements were performed with a CHI660A electrochemical workstation. The exposed area of the working electrode was 0.26 cm². All CV experiments were carried out in a conventional three-electrode cell at 17 ± 1 °C. A saturated calomel

electrode (SCE) and a Pt wire were employed as reference and counter electrodes, respectively. XPS spectra were measured on a VG ESCALAB 5 multitechnique electron spectrometer.

Financial support from the Ministry of Science and Technology, the National Natural Science Foundation of China and the Post-doctoral Foundation of China is greatly appreciated.

- [1] a) S. J. Trans, M. H. Devoret, H. J. Dai, A. Thess, R. E. Smalley, L. J. Geerligs, C. Dekker, *Nature* **1997**, *386*, 474–477; b) M. Bockrath, D. H. Cobden, P. L. McEuen, N. G. Chopra, A. Zettl, A. Thess, R. E. Smalley, *Science* **1997**, *275*, 1922–1925; c) S. J. Trans, A. R. M. Verschueren, C. Dekker, *Nature* **1998**, *393*, 49–52.
- [2] a) J. Kong, N. R. Franklin, C. Zhou, G. M. Chapline, S. Peng, D. Kyeongjae, H. J. Dai, *Science* **2000**, *287*, 622–625; b) P. G. Collins, K. Bradley, M. Ishigami, A. Zettl, *Science* **2000**, *287*, 1801–1804.
- [3] S. S. Wong, A. T. Woolley, E. Joselevich, C. L. Cheung, C. M. Lieber, *J. Am. Chem. Soc.* **1998**, *120*, 8557–8558.
- [4] a) D. Chattopadhyay, I. Galeska, F. Papadimitrakopoulos, *J. Am. Chem. Soc.* **2001**, *123*, 9451–9452; b) Z. F. Liu, Z. Y. Shen, T. Zhu, S. F. Huo, L. Z. Ying, Z. J. Shi, Z. N. Gu, *Langmuir* **2000**, *16*, 3569–3573; c) B. Wu, J. Zhang, Z. Wei, S. M. Cai, Z. F. Liu, *J. Phys. Chem. B* **2001**, *105*, 5075–5078.
- [5] J. K. Campbell, L. Sun, R. M. Crooks, *J. Am. Chem. Soc.* **1999**, *121*, 3779–3780.
- [6] a) P. J. Britto, K. S. V. Santhanam, P. M. Ajayan, *Bioelectrochem. Bioenerg.* **1996**, *41*, 121–125; b) J. J. Davis, R. J. Coles, H. A. O. Hill, *J. Electroanal. Chem.* **1997**, *440*, 279–282.
- [7] J. Chen, M. A. Hamon, H. Hu, Y. Chen, A. M. Rao, P. C. Eklund, R. C. Haddon, *Science* **1998**, *282*, 95–98.
- [8] D. R. Lloyd, C. M. Burns, *J. Polym. Sci.* **1979**, *17*, 3473–3483.
- [9] S. S. Wong, A. T. Woolley, T. W. Odom, J.-L. Huang, P. Kim, D. V. Vezenov, C. M. Lieber, *Appl. Phys. Lett.* **1998**, *73*, 3465–3467.
- [10] G. S. Duesberg, I. Loa, M. Burghard, K. Syassen, S. Roth, *Phys. Rev. Lett.* **2000**, *85*, 5436–5439.
- [11] K. Takehara, H. Takemura, Y. Ide, *Electrochim. Acta* **1994**, *39*, 817–822.
- [12] C. Amatore, J. M. Saveant, D. Tessier, *J. Electroanal. Chem.* **1983**, *147*, 39–51.
- [13] C. E. D. Chidsey, *Science* **1991**, *251*, 919–922.
- [14] A. M. Cassell, J. A. Raymakers, J. Kong, H. Dai, *J. Phys. Chem. B* **1999**, *103*, 6484–6492.
- [15] J. Liu, A. G. Rinzler, H. Dai, J. H. Hafner, R. K. Bradley, P. J. Boul, A. Lu, T. Iverson, K. Shelimov, C. B. Huffman, F. Rodriguez-Macias, Y.-S. Shon, T. R. Lee, D. T. Colbert, R. E. Smalley, *Science* **1998**, *280*, 1253–1256.

Received: July 25, 2002 [Z464]